

Decay of  $^{127}\text{In}$  and  $^{129}\text{In}$ H. Gausemel,<sup>1</sup> B. Fogelberg,<sup>2</sup> T. Engeland,<sup>3</sup> M. Hjorth-Jensen,<sup>3</sup> P. Hoff,<sup>1</sup> H. Mach,<sup>2</sup> K. A. Mezilev,<sup>4</sup> and J. P. Omtvedt<sup>1</sup><sup>1</sup>*Department of Chemistry, University of Oslo, P.O. Box 1033 Blindern N-0315 Oslo, Norway*<sup>2</sup>*Department of Radiation Sciences, University of Uppsala, S-61182 Nyköping, Sweden*<sup>3</sup>*Department of Physics, University of Oslo, P.O. Box 1048 Blindern, N-0316 Oslo, Norway*<sup>4</sup>*Petersburg Nuclear Physics Institute, Gatchina, St. Petersburg 188350, Russia*

(Received 5 December 2003; published 14 May 2004)

The decay properties of  $^{127}\text{In}$  and  $^{129}\text{In}$  have been investigated using Isotope Separation On-Line (ISOL) produced samples. In both  $^{127}\text{In}$  and  $^{129}\text{In}$  new  $\beta$ -decaying isomeric states were observed, with half-lives of  $1.04 \pm 0.10$  and  $0.67 \pm 0.10$  s, respectively, in addition to the previously known isomers of single proton hole  $p_{1/2}$  and  $g_{9/2}$  character.  $Q_\beta$  measurements show that the new isomeric states are present at energies approaching 2 MeV above the ground states. The level schemes of  $^{127}\text{Sn}$  and  $^{129}\text{Sn}$  have been considerably extended. The modes of feeding and decay of the two  $\mu\text{s}$  isomers in each of the Sn nuclei are fully elucidated, including new half-life determinations. Shell model calculations on  $^{127}\text{Sn}$  and  $^{129}\text{Sn}$  were performed, giving results in good agreement with the new data.

DOI: 10.1103/PhysRevC.69.054307

PACS number(s): 21.10.-k, 23.20.Lv, 21.60.Cs, 27.60.+j

## I. INTRODUCTION

In the vicinity of the doubly magic  $^{132}\text{Sn}$ , the unique parity orbitals situated just below shell closure give rise to a multitude of high spin states of three-quasiparticle (3qp) nature in the odd-mass nuclides. The present study was initiated in order to search for new  $\beta$ -decaying isomers of  $^{127}\text{In}$  and  $^{129}\text{In}$ . Low-lying 3qp states will often have a unique structure and their properties are of importance for tests of theoretical calculations. A well known example is given by the  $\beta$ -decaying isomer at 4.3 MeV in  $^{131}\text{In}$  [1], which populates high spin states at a similar energy in  $^{131}\text{Sn}$ . The high excitation energies here are a consequence of the single-hole character of these nuclides. Further away from the shell closure, many of the high spin 2qp and 3qp states are found in the 2 MeV region.

Near the middle of the neutron shell, heavy ion reactions have proved to be efficient for the population of such states. Some years ago Mayer *et al.* [2], observed microsecond yrast isomers populated in deep inelastic collisions leading to  $^{119,121,123}\text{Sn}$ . In the more neutron-rich nuclides, the population of high spin states is more efficiently achieved in fission. This mode of excitation has been used, for example, by Pinston *et al.* [3–5] to identify  $\mu\text{s}$  yrast isomers in  $^{125,127,129}\text{Sn}$  and in the heavy Sb isotopes. Even more long-lived yrast traps with millisecond life times were found in  $^{131}\text{Te}$  and  $^{125,129}\text{In}$  during the early course of the current work [6]. There were thus good reasons to expect the presence of  $\beta$ -decaying isomers in  $^{127,129}\text{In}$ , as well as strong indications for such isomers in previous data as pointed out by Pinston *et al.* [3].

An additional motivation for this work was that more detailed information was desired on the structures of  $^{127}\text{Sn}$  and  $^{129}\text{Sn}$ , two rather simple systems with five and three neutron-holes. Investigations of these nuclei have previously been reported by DeGeer and Holm [7] from early works at our laboratory, and the compilations in Nuclear Data Sheets [8,9] are mainly based on the study by these authors.

In the present work, a comprehensive study of the  $^{127}\text{In}$  and  $^{129}\text{In}$  decays is described. We have studied the radiations

following the  $\beta$  decays by multispectrum scaling (MSS) of singles spectra and by  $\gamma\gamma$ - and  $\beta\gamma$ -coincidence measurements. The MSS data were used to determine the  $\beta$ -decay half-life associated with each  $\gamma$  transition, while the  $\gamma\gamma$  measurements were used to verify and extend the level schemes of  $^{127}\text{Sn}$  and  $^{129}\text{Sn}$ . The  $\beta\gamma$ -coincidence spectroscopy measurements have been used to find the end point energies of individual  $\beta$  transitions to selected final levels, which were needed for the determination of the excitation energies of the new isomeric states. The new data on the structures of  $^{127,129}\text{Sn}$  are interpreted by comparison with results from a shell model calculation using realistic effective interactions.

## II. EXPERIMENTAL DETAILS

The measurements were performed at the OSIRIS fission product mass separator at Studsvik, Sweden. For details on this facility, see Ref. [10] and references therein.

The  $A=127$  and  $A=129$  activities were obtained from thermal neutron-induced fission of a  $^{235}\text{U}$  carbide target inside the combined target and ion source ANUBIS [11]. During the measurements of singles data, surface ionization was used to select the element In and thereby suppress the daughter activities. For the coincidence measurements, plasma ionization was chosen in order to obtain somewhat higher yields. After mass separation, the  $A=127$  or  $A=129$  beam was collected on a movable Al-coated Mylar tape in the center of the measuring station.

The experimental setup for the  $\gamma\gamma$  coincidences consisted of three Ge detectors of which one was a low energy photon (LEP). Three Ge detectors were also used for the  $Q_\beta$  measurement, where the LEP detector now was used as a  $\beta$  spectrometer. In this latter case the LEP could “view” the beam collection spot through two thin windows of Al and Be, as described in Ref. [12]. The LEP electronics was set to accept energies up to about 16 MeV.

The  $\gamma$ -ray MSS measurements were performed in a repeated cycle consisting of eight sequential time groups, each

yielding a spectrum recorded with a Ge detector. The cycle was started after removal of the old sample by the tape transport system. The first time group was a background radiation measurement with the beam deflected. The second and third groups were collected while the beam was continuously deposited on the tape. The remaining spectra were collected with the beam deflected, in order to study the decaying activities. In the case of  $A=127$ , the group time of the spectra was 1.0 s, which gives suitable conditions for studies of the  $\beta$  decays of the two known isomers in  $^{127}\text{In}$ , with half-lives of 1.09 and 3.67 s. The isobar  $^{127}\text{Cd}$  was also present, however, with a much lower yield and having a short half-life of 0.43 s, which was easy to differentiate from the In half-lives. For  $A=129$ , a group time of 0.5 s was chosen, suited for the  $\beta$  decay of the two known isomers in  $^{129}\text{In}$ , with half-lives of 0.61 and 1.23 s. Other  $A=127$  and  $A=129$  isobars present in the samples have half-lives considerably longer than these values.

The energy calibrations were obtained by using well known  $\gamma$  energies from  $^{127}\text{Sn}$  and  $^{129}\text{Sn}$  as internal reference points as well as external sources of  $^{152}\text{Eu}$ , Pb x rays, and the 6128 keV line from  $^{16}\text{O}$ . Additional singles spectra of calibrated reference sources were also recorded for the determination of detector efficiencies.

### III. EXPERIMENTAL RESULTS

#### A. Data analysis

The general features of the decays of  $^{127}\text{In}$  and  $^{129}\text{In}$  are quite similar. As a consequence, similar analysis methods were used. Since the data clearly showed the presence of a new  $\beta$ -decaying isomer in both cases, an immediate concern was how to assign the observed transitions to each of the isomers present. From the MSS data, many transitions could be identified as belonging to the decay of either the two high spin isomers or to the low spin isomer in In, the latter with a significantly longer half-life. Separation of the two high spin isomers was not possible from the MSS data alone, since in both  $A=127$  and  $A=129$  the half-life of the new isomer turned out to be practically identical to the half-life of the known  $9/2^+$  ground state. However, some of the transitions have previously been observed to follow the decays of high spin states with  $\mu\text{s}$  half-lives [3,4], and could therefore be assigned to the new high spin isomer. The  $\gamma\gamma$  coincidences were then used to assign the weaker transitions and to resolve transitions appearing in the decays of more than one isomer. The division of intensity and assignment of such lines was cross-checked with the results from the MSS analysis. In addition to the prompt  $\gamma\gamma$  coincidences, delayed coincidences were also investigated in order to link the transitions above the isomeric states in Sn with the transitions below. This was possible since the time-to-amplitude converter (TAC) gate was chosen to be 5  $\mu\text{s}$  wide, and although the delayed signals are weak, the coincidences were unambiguous.

The  $\beta\gamma$ -coincidence data, which were taken using a 20  $\mu\text{s}$  TAC range, were analyzed with respect to determinations of the end point energies of selected  $\beta$  transitions. The  $\beta$  transitions from the decays of the new high spin In isomers were

TABLE I. Results from the measurement of the total decay energies of  $^{127,129}\text{In}$ .

$\beta$ -decaying state	Derived $Q_\beta$ (keV) <sup>a</sup>	Excitation energy of initial state (keV)
$^{127}\text{In } 9/2^+$	6579(20)	0
$1/2^-$	6999(63)	420(65)
$21/2^-$	8442(56)	1863(58)
$^{129}\text{In } 9/2^+$	7780(26)	0
$1/2^-$	8149(38)	369(46)
$23/2^-$	9410(50)	1630(56)

<sup>a</sup>Here and in the following tables, all uncertainties are given in units of the last digit.

initially analyzed by choosing a delayed TAC window and  $\gamma$ -ray gates on the transitions cascading from the  $\mu\text{s}$  isomers in the Sn daughter nuclei. After having established that the main  $\beta$  transitions populate levels at higher energies, the final  $\beta$ -spectra end point energies were derived from sums of spectra projected using prompt gates on the  $\gamma$  rays depopulating the 3605 and 3993 keV states in  $^{127}\text{Sn}$  and  $^{129}\text{Sn}$ , respectively. Additional prompt  $\gamma$ -ray gates were used to determine end point energies of strong transitions in the decays of the ground states and  $1/2^-$  isomers of the In nuclei. The excitation energies of the new In isomers were determined from the derived  $Q_\beta$  values. The results of the  $Q_\beta$  measurements are shown in Table I.

The  $\beta\gamma$ -data set gave the possibility of studying the half-lives of the high spin states in the Sn nuclei by projecting TAC spectra gated both by  $\beta$  particles and the depopulating  $\gamma$ -transitions in Sn. Examples of TAC spectra are given in Figs. 1 and 2. Our data showed the presence of two  $\mu\text{s}$  isomers in both  $^{127}\text{Sn}$  and  $^{129}\text{Sn}$ . Table II shows a comparison between the half-lives found in this study and previously at Institute Laue-Langevin (ILL), Grenoble [3,4].

We made one attempt to determine absolute  $\gamma$ -ray intensities in the decays of the In isomers by a simultaneous MSS measurement of  $\gamma$  rays and  $\beta$  particles. The results were not more accurate than the values already reported by Rudstam [13]. The results of Rudstam are therefore used here, with a small correction for the presence of the new high spin  $\beta$ -decaying isomers. The data indicate that there is no strong  $\beta$  feeding of the Sn  $h_{11/2}$  states from the In  $g_{9/2}$  ground states. We have neglected these possible but unobserved  $\beta$  transitions when deducing the absolute intensities in the In ground state decays. (The  $\beta$ -transition intensities may amount to a few percent as discussed later in text.) The intensities of the strong first forbidden  $\beta$  transitions feeding the Sn  $d_{3/2}$  and  $s_{1/2}$  states are given in Table III as obtained from the data of Ref. [13] and the decay schemes presented here. Data for the corresponding transitions in the decay of the single proton hole nucleus  $^{131}\text{In}$  are included in Table III for comparison. Regarding the  $\beta$  decays of the new high spin In isomers, we note that the  $\gamma$ -ray cascades in the Sn nuclei are ultimately concentrated into 2–3 transitions leading to the  $h_{11/2}$  states. The combined intensities of these transitions have been taken to represent 100% of the respective decay. It should be noted

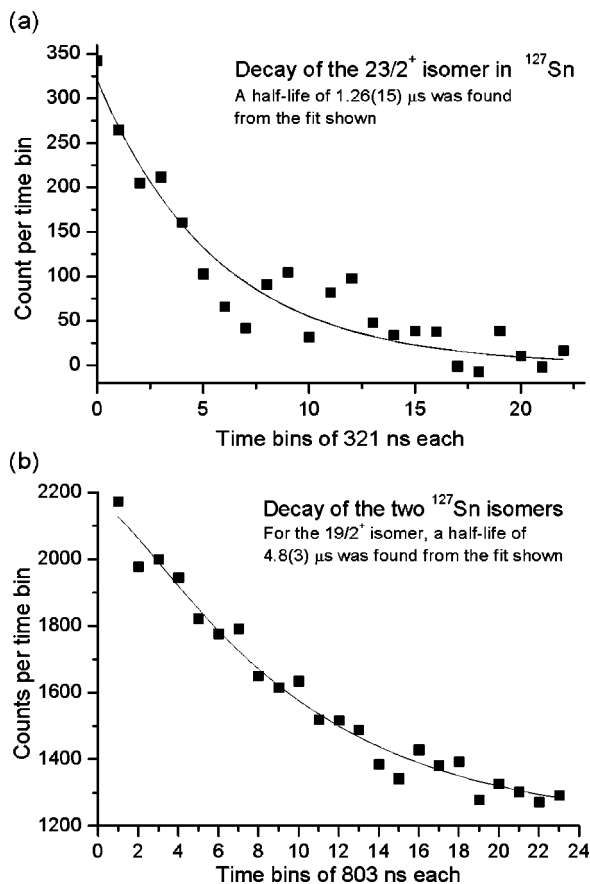


FIG. 1. (a) A TAC spectrum obtained between  $\beta$ -particle signals from a LEP spectrometer and events from the 104 keV transition in  $^{127}\text{Sn}$  detected in a Ge detector. A half-life of  $1.26(15) \mu\text{s}$  was deduced for the  $23/2^+$  isomer from the data shown. The coincident background was subtracted from the spectrum. (b) A TAC spectrum obtained as above, but by gating on the 715 keV transition, containing half-life contributions from both isomers. The half-life of the lower isomer was deduced as  $4.8(3) \mu\text{s}$  by using the value from Fig. 1(a) for the upper isomer.

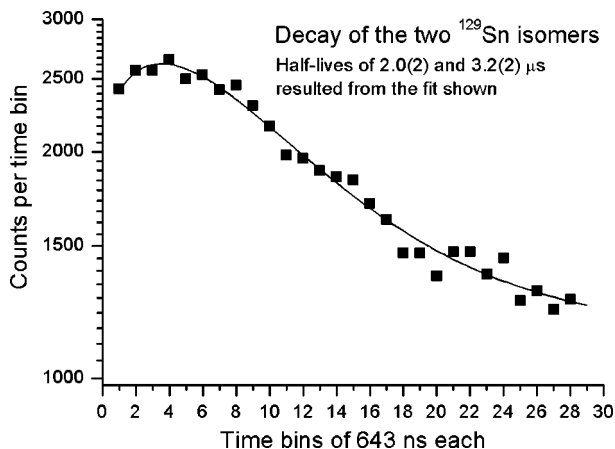


FIG. 2. A TAC spectrum gated on the 382 and 570 keV transitions in  $^{129}\text{Sn}$ , thereby showing half-life contributions from both isomers. An analysis of the growth and decay shape of the spectrum resulted in the half-life values shown.

TABLE II. Comparison of the half-lives of  $E2$  isomers in Sn measured in the present and previous [3,4] works.

State	Present	Previous
$^{127}\text{Sn } 23/2^+$ (1931 keV)	$1.26 (15) \mu\text{s}$	
$^{127}\text{Sn } 19/2^+$ (1827 keV)	$4.8 (3) \mu\text{s}$	$4.5 (3) \mu\text{s}$
$^{129}\text{Sn } 23/2^+$ (1801 keV)	$2.0 (2) \mu\text{s}$	$2.4 (2) \mu\text{s}$
$^{129}\text{Sn } 19/2^+$ (1760 keV)	$3.2 (2) \mu\text{s}$	$3.6 (2) \mu\text{s}$

that we observe an imbalance of the  $\gamma$ -ray intensities for the transitions feeding and depopulating the lowest excited levels ( $13/2^-$  and  $15/2^-$ ) in each of these cascades. Lacking other plausible explanations for the imbalances, we suggest that the cause is a feeding of these excited states by unobserved  $\gamma$  rays of relatively high energies.

### B. Systematics and spin assignments

The ground states of all known odd In nuclei are formed by the  $g_{9/2}$  proton hole state. In the neutron rich isotopes, this state decays with a strong Gamow-Teller (GT) transition, with a  $\log ft$  of about 4.4, to the neutron  $g_{7/2}$  state in the Sn daughter. The  $\gamma$  decay of the latter state is dominated by an  $E2$  transition to the neutron  $d_{3/2}$  level. This decay sequence is a prominent feature also in the In  $9/2^+$  decays studied here. The  $\gamma$  rays corresponding to the  $g_{7/2} \rightarrow d_{3/2}$  transitions dominate the spectra. In analogy with DeGeer and Holm [7], we adopt these  $7/2^+$  and  $3/2^+$  assignments as firm. (In  $^{129}\text{Sn}$ , the  $7/2^+$  strength is split on two states having similar decay patterns.) We also adopt as firm the  $1/2^+$  and  $3/2^+$  assignments given by Ref. [7] for the two lowest low spin states populated by the strong first forbidden transitions in the decays of the  $^{127,129}\text{In } p_{1/2}$  isomeric states. The spins and parities of several additional levels in  $^{127,129}\text{Sn}$  then follow from application of the selection rules for  $\beta$  and  $\gamma$  transitions.

A strong GT branch with a  $\log ft$  of 4.4–4.5 is observed in the decays of each of the high spin isomers found presently in  $^{127,129}\text{In}$ . These branches are interpreted to have the same character as the  $\pi g_{9/2}^{-1} \rightarrow \nu g_{7/2}^{-1}$  transitions mentioned above. However, the subsequent  $\gamma$  decays of the populated levels are not dominated by the corresponding  $E2$  transitions, because the final states in these  $\beta$  decays are highly excited, opening possibilities for competition from much faster  $E1$  decays. The most likely shell model configuration for the high spin In isomers is a  $g_{9/2}$  proton hole coupled to two neutron holes in the  $h_{11/2}$  and  $d_{3/2}$  orbitals (the latter is equivalent to the  $7^-$  two-neutron core states in  $^{128}\text{Sn}$  and  $^{130}\text{Sn}$ ). The GT decay effectively transforms the  $g_{9/2}$  proton

TABLE III. Intensities in %/decay of the strong first forbidden transitions following the decays of the  $p_{1/2}$  isomers of the heavy In isotopes. The relative uncertainties in the values are about 10–20%.

Final state\mass	127	129	131
$p_{3/2}$	50	77	95
$s_{1/2}$	34	17	3

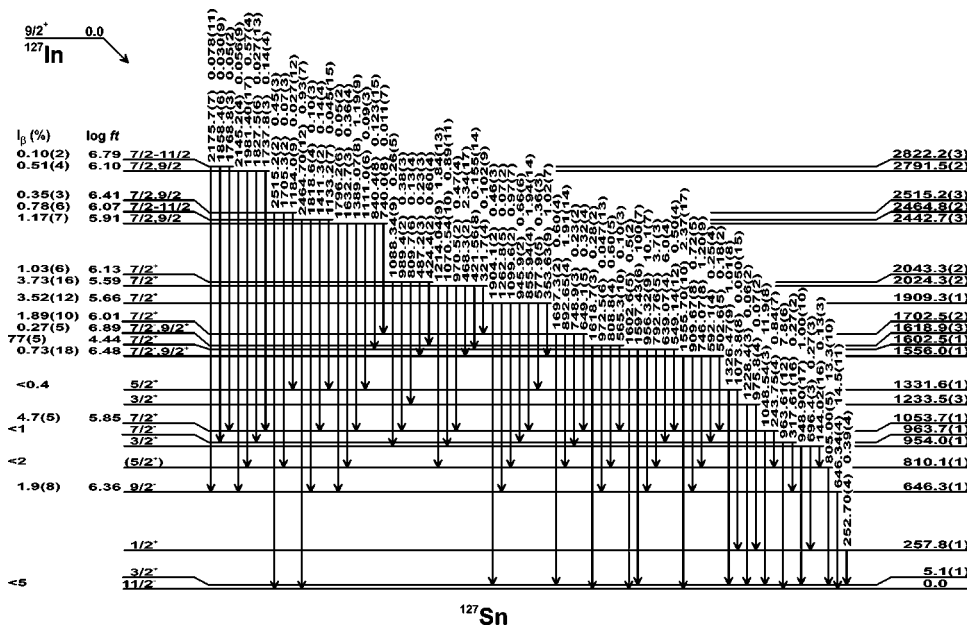


FIG. 3. Levels of  $^{127}\text{Sn}$  populated in the decay of the  $9/2^+$  ground state of  $^{127}\text{In}$  ( $t_{1/2}=1.09$  s). Absolute  $\gamma$  intensities in % are obtained by multiplication with 0.64. See the text for details.

hole to a  $g_{7/2}$  neutron hole in the final state configuration. In the case of  $^{127}\text{Sn}$ , rather strong  $\beta$  transitions are populating both of the  $19/2^+$  and  $23/2^+$  microsecond isomers (discussed below), indicating a  $21/2^-$  assignment for the high spin  $\beta$ -decaying parent state. The final state of the GT transition then has  $J^\pi=19/2^-$ , which is fully consistent with the observed  $\gamma$ -ray branchings. The strong  $\gamma$  decay of the 3605 keV state to a well established  $15/2^-$  level practically ensures the suggested negative parity, and hence also a negative parity of the  $^{127}\text{In}$  isomer. One should note that the  $E2$  transition corresponding to  $g_{7/2} \rightarrow d_{3/2}$  now proceeds between configurations having three neutron holes in the  $g_{7/2}$ ,  $h_{11/2}$ , and  $d_{3/2}$  orbitals (initial) and the  $h_{11/2}$  plus  $d_{3/2}^2$  orbitals (fi-

nal). The latter state is in practice a member of the multiplet formed by the  $h_{11/2}$  neutron hole coupled to the  $2^+$  phonon of the core, and is found with  $J^\pi=15/2^-$  at 1094.7 keV. In the case of the  $^{129}\text{In}$  high spin decay, the final state of the GT transition (at 3993 keV in  $^{129}\text{Sn}$ ) decays by strong  $E1$  transitions to both the  $19/2^+$  and the  $23/2^+$   $\mu\text{s}$  isomers in  $^{129}\text{Sn}$ . The 3993 keV state is thus  $21/2^-$ , corresponding to the maximum alignment of this three-neutron configuration. An  $E2$  decay to the  $15/2^-$  phonon state is therefore not possible as in  $^{127}\text{Sn}$ . The high spin isomer in  $^{129}\text{In}$  must then be  $23/2^-$  since these fast GT transitions connect  $J$  and  $J-1$  states.

The following two sections give some details on the deduced properties of the  $A=127$  and  $A=129$  In to Sn decays,

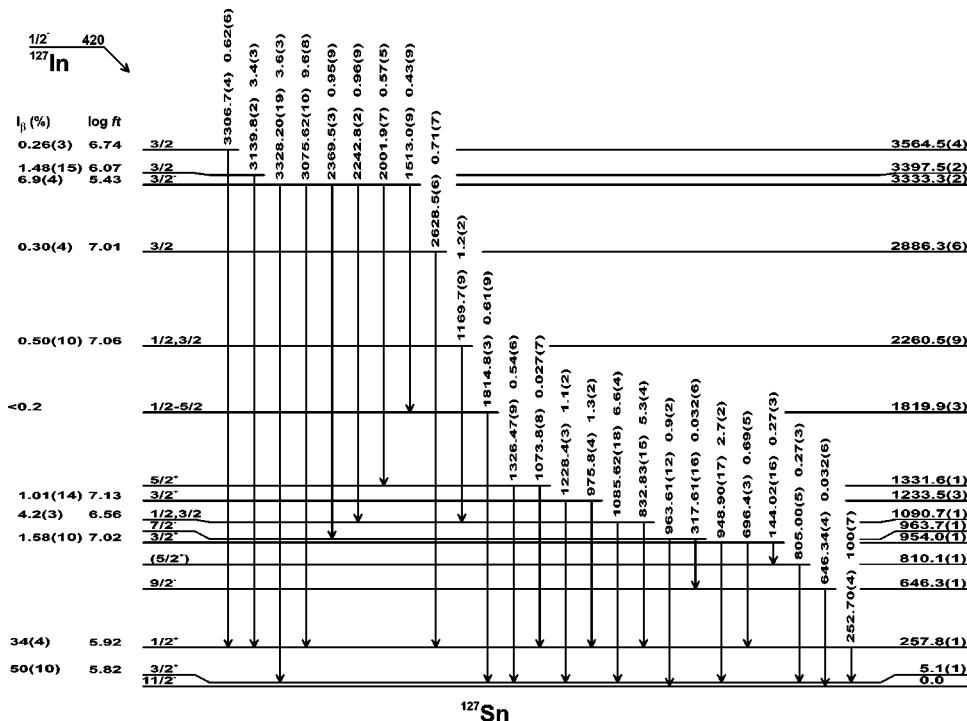


FIG. 4. Levels of  $^{127}\text{Sn}$  populated in the decay of the  $1/2^-$  isomer of  $^{127}\text{In}$  ( $t_{1/2}=3.67$  s). Absolute  $\gamma$  intensities in % are obtained by multiplication with 0.43. See the text for details.

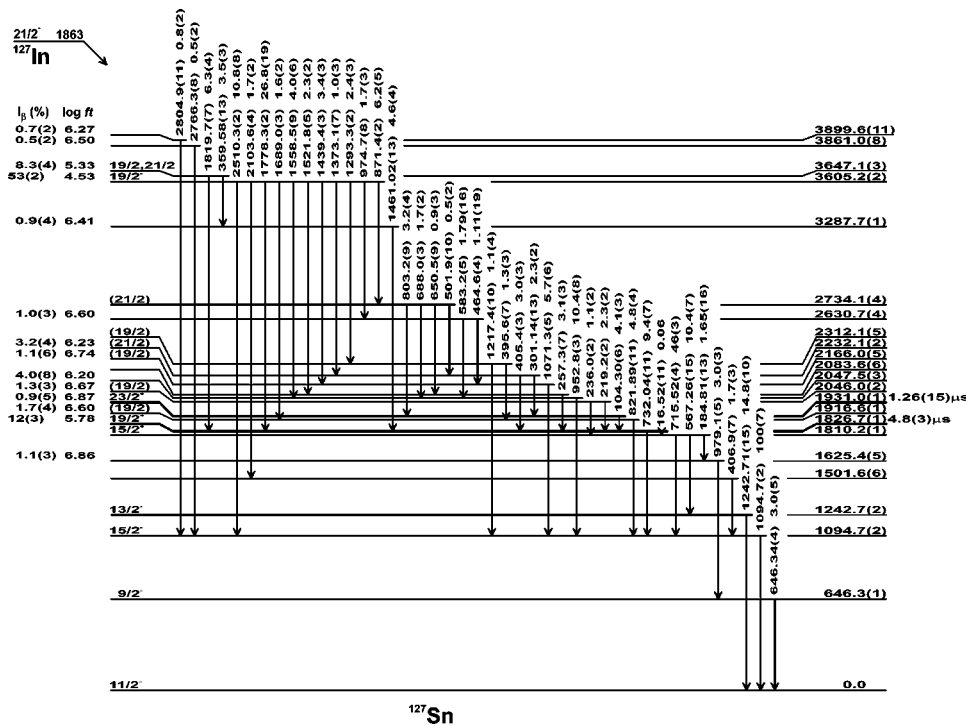


FIG. 5. Levels of  $^{127}\text{Sn}$  populated in the decay of the  $21/2^-$  isomer of  $^{127}\text{In}$  ( $t_{1/2}=1.04\pm 0.10$  s). Absolute  $\gamma$  intensities in % are obtained by multiplication with 0.85. The  $\gamma$  line of 16.52 keV was not observed, and both the total intensity of 57.3 units and the transition energy were deduced from the level scheme. For the levels at 1094.7 and 1242.7 keV, unobserved  $\gamma$  feeding is likely, and the true  $\beta$  feeding is assumed to be zero. The ordering of the  $\gamma$  cascade of 406.9 and 2103.6 keV may be interchanged, as the position is not clear. See the text for further details.

and is followed by a summary of a shell model calculation describing the structure of the Sn nuclei.

C. A = 127

The levels of  $^{127}\text{Sn}$  populated in the decays of the three In isomers are shown in Figs. 3–5. The previously proposed [7] excited states are confirmed and 34 additional levels have been established presently. A total of 126 transitions were placed in the decay schemes. One should note the imbalance mentioned above regarding the  $\gamma$ -ray intensities feeding and

depopulating the 1095 and 1243 keV states, and also that the position of the 1501 keV level is uncertain since the order of the 407 and 2104 keV transitions is not known.

Four states of neutron hole character ( $h_{11/2}$ ,  $d_{3/2}$ ,  $s_{1/2}$ , and  $g_{7/2}$ ) are identified at 0, 5, 258, and 1603 keV in agreement with the results of DeGeer and Holm [7]. A  $5/2^+$  state identified by us at 1332 keV is likely to represent the, so far missing, neutron hole  $d_{5/2}$  state. The excitation energy agrees with expectations from systematics, and the  $E2$  and  $M1$  branching of the transitions in the  $\gamma$ -ray decay to lower-lying hole states is in fair agreement with the observed decay prop-

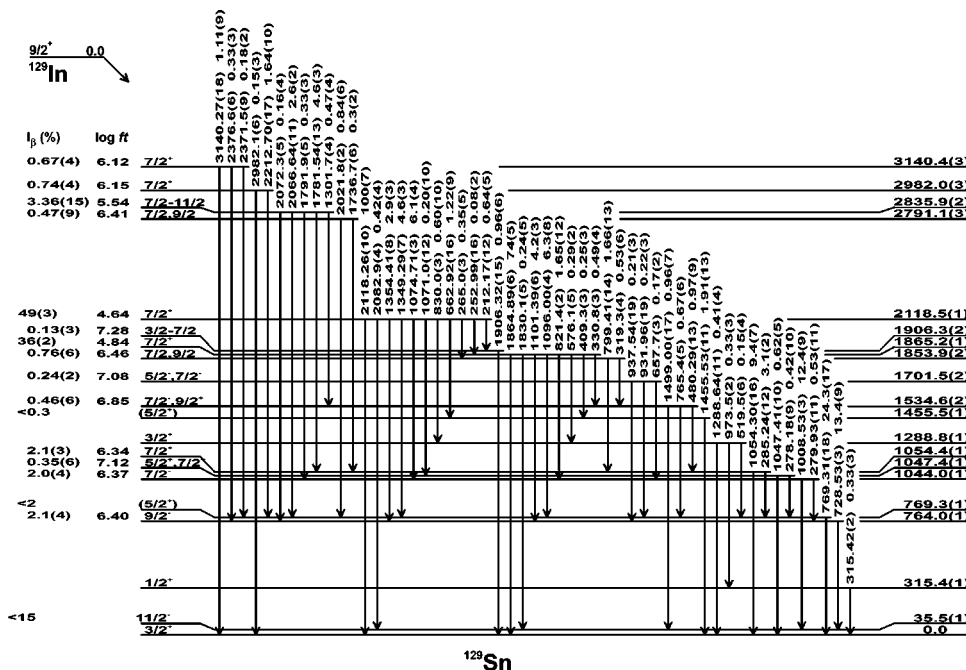


FIG. 6. Levels of  $^{129}\text{Sn}$  populated in the decay of the  $9/2^+$  ground state of  $^{129}\text{In}$  ( $t_{1/2}=0.61$  s). Absolute  $\gamma$  intensities in % are obtained by multiplication with 0.42. The level at 1047.4 keV has spin  $7/2^+$  if  $\beta$  feeding exists. See the text for details.

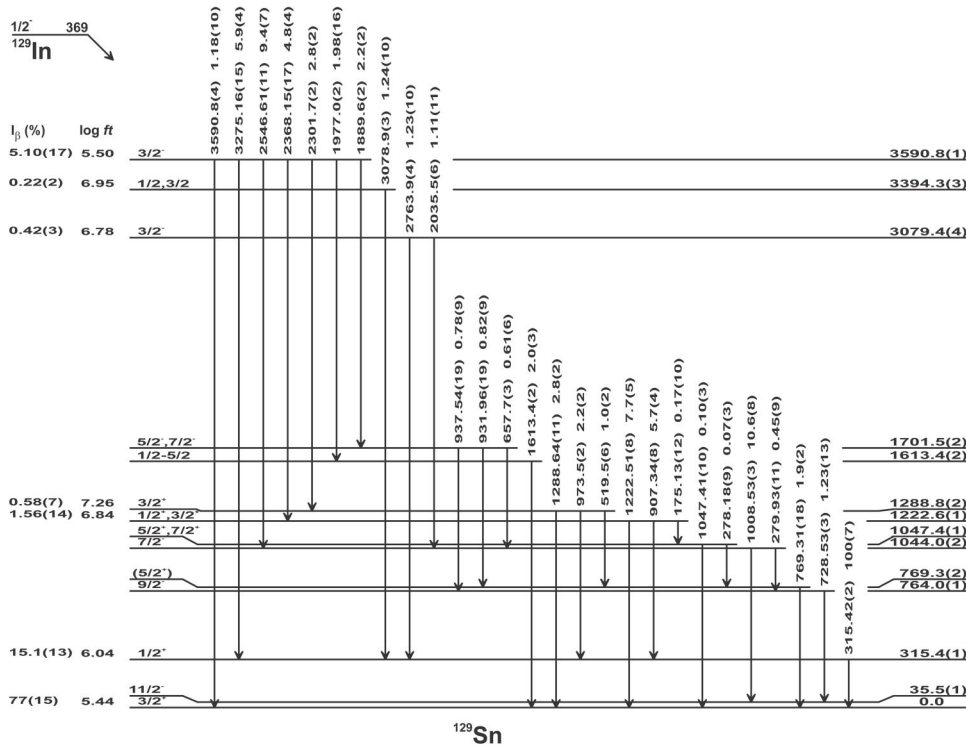


FIG. 7. Levels of  $^{129}\text{Sn}$  populated in the decay of the  $1/2^-$  isomer of  $^{129}\text{In}$  ( $t_{1/2}=1.23$  s). Absolute  $\gamma$  intensities in % are obtained by multiplication with 0.18. The level at 1047.4 keV has spin  $7/2^+$  if  $\beta$  feeding exists. See the text for details.

erties of the corresponding  $f_{7/2}$  neutron hole state in  $^{207}\text{Pb}$ . The four negative parity states ( $7/2^-$ ,  $9/2^-$ ,  $13/2^-$ , and  $15/2^-$ ) due to the coupling of the  $h_{11/2}$  hole state to the  $2^+$  core phonon are found in the range 646 to 1243 keV as seen in the decay schemes. Positive parity core coupled states due to  $d_{3/2}$  and  $s_{1/2}$  are present at 810, 954, 1053, 1090, 1233, and 1332 keV. As mentioned above, the latter of these levels is

likely to have a strong component of the neutron hole  $d_{5/2}$  state.

The higher-lying levels are difficult to characterize, except for some of the high spin 3qp states. The  $19/2^+$  isomeric state at 1826 keV in  $^{127}\text{Sn}$  was reported by Pinston *et al.* [3]. These authors proposed that the isomer could be explained as a  $h_{11/2}$  neutron hole coupled with the  $5^-$  core state. Our

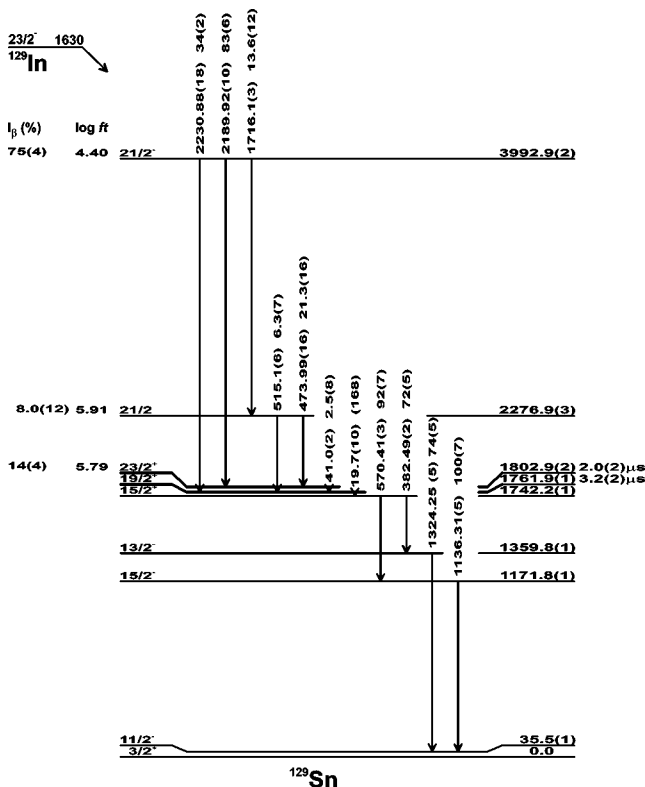


FIG. 8. Levels of  $^{129}\text{Sn}$  populated in the decay of the  $23/2^-$  isomer of  $^{129}\text{In}$  ( $t_{1/2}=0.67\pm 0.10$  s). Absolute  $\gamma$  intensities in % are obtained by multiplication with 0.58. For the  $\gamma$  line of 19.7 keV, the total intensity of about 168 units was deduced from the level scheme. For the level at 1171.8 keV, unobserved  $\gamma$  feeding is likely, and the true  $\beta$  feeding is assumed to be zero. Regarding the  $\beta$  feeding of the 1761.9 and 1802.9 levels, only the sum of the  $\beta$  feeding was obtained experimentally. See the text for further details.

TABLE IV. Results from the shell model calculations for  $^{127}\text{Sn}$  compared to the experimental data.

$J^\pi$	$E_{\text{calc}}$ (MeV)	$E_{\text{exp}}$ (MeV)
$11/2_1^-$	0	0
$3/2_1^+$	0.032	0.005
$1/2_1^+$	0.172	0.258
$9/2_1^-$	0.793	0.646
$7/2_1^-$	0.896	0.964
$3/2_2^+$	0.937	0.954
$5/2_1^+$	0.942	0.810 <sup>a</sup>
$15/2_1^-$	1.075	1.095
$5/2_2^+$	1.288	1.331
$1/2_2^+$	1.338	
$7/2_1^+$	1.341	1.054
$3/2_3^+$	1.357	1.233
$13/2_1^-$	1.418	1.243
$5/2_1^-$	1.447	
$7/2_2^+$	1.519	1.603
$11/2_1^-$	1.533	
$5/2_3^+$	1.631	
$13/2_2^-$	1.655	
$3/2_4^+$	1.676	
$3/2_1^-$	1.696	
$9/2_1^+$	1.738	
$1/2_3^+$	1.762	
$7/2_3^+$	1.771	1.702
$11/2_2^-$	1.786	
$9/2_2^-$	1.814	
$11/2_1^+$	1.888	
$11/2_3^-$	1.924	
$19/2_1^-$	1.984	1.917 <sup>a</sup>
$19/2_1^+$	2.017	1.827
$9/2_3^-$	2.025	
$7/2_2^-$	2.029	
$15/2_1^+$	2.038	1.810
$9/2_2^+$	2.054	
$3/2_5^+$	2.057	
$13/2_3^-$	2.062	
$7/2_4^+$	2.066	1.909
$5/2_2^-$	2.068	
$5/2_4^+$	2.068	
$7/2_5^+$	2.094	2.024
$13/2_1^+$	2.112	
$7/2_3^-$	2.118	
$23/2_1^+$	2.123	1.931
$5/2_5^+$	2.134	
$15/2_2^-$	2.137	
$17/2_1^-$	2.179	
$19/2_2^+$	2.197	
$5/2_6^+$	2.260	
$13/2_4^-$	2.261	
$17/2_1^+$	2.276	
$9/2_3^+$	2.289	
$15/2_3^-$	2.292	
$15/2_2^+$	2.300	

<sup>a</sup>Spin not conclusively decided experimentally.

TABLE V. Results from the shell model calculations for  $^{129}\text{Sn}$  compared to the experimental data.

$J^\pi$	$E_{\text{calc}}$ (MeV)	$E_{\text{exp}}$ (MeV)
$3/2_1^+$	0.000	0
$11/2_1^-$	0.052	0.036
$1/2_1^+$	0.307	0.315
$5/2_1^+$	0.992	0.769
$7/2_1^-$	1.060	1.044
$9/2_1^-$	1.178	0.764
$3/2_2^+$	1.252	1.222 <sup>a</sup>
$7/2_1^+$	1.262	1.054
$15/2_1^-$	1.273	1.172
$1/2_2^+$	1.442	
$11/2_2^-$	1.464	
$3/2_3^+$	1.494	1.289 <sup>a</sup>
$5/2_2^+$	1.520	1.455 <sup>a</sup>
$11/2_1^+$	1.692	
$13/2_1^-$	1.704	1.360
$9/2_1^+$	1.730	
$5/2_3^+$	1.755	
$15/2_1^+$	1.812	1.742
$19/2_1^+$	1.836	1.761
$13/2_2^-$	1.865	
$23/2_1^+$	1.874	1.801
$3/2_4^+$	1.912	
$7/2_2^-$	1.944	
$7/2_2^+$	1.970	1.865
$5/2_1^-$	2.002	
$15/2_2^-$	2.045	
$13/2_1^+$	2.053	
$7/2_3^+$	2.078	2.118
$11/2_3^-$	2.082	
$9/2_2^-$	2.091	
$3/2_1^-$	2.104	3.079
$5/2_4^+$	2.112	
$13/2_3^-$	2.126	
$9/2_2^+$	2.134	
$11/2_4^-$	2.141	
$17/2_1^+$	2.256	
$13/2_2^+$	2.275	
$9/2_3^-$	2.296	
$15/2_3^-$	2.302	
$7/2_4^+$	2.304	2.984
$19/2_2^+$	2.310	
$17/2_2^+$	2.335	
$5/2_5^+$	2.340	
$3/2_5^+$	2.351	
$19/2_1^-$	2.372	
$11/2_5^-$	2.384	
$17/2_1^-$	2.425	
$1/2_3^+$	2.430	
$11/2_2^+$	2.455	
$15/2_2^+$	2.456	
$15/2_3^-$	2.477	
$11/2_3^+$	2.509	
$11/2_6^-$	2.518	
$21/2_1^+$	2.531	

<sup>a</sup>Spin not conclusively decided experimentally.

present investigation has revealed an additional isomeric state at 1931 keV, decaying by a 104 keV transition to the lower isomer. The half-life of this second isomer was found to be  $1.26(15) \mu\text{s}$ , see Table II, which is compatible with an  $E2$  multipolarity of the 104 keV transition. The spin of the new isomer is thus most likely  $23/2$ . The structure of the state can be seen as a coupling of the  $h_{11/2}$  neutron hole to the  $7^-$  core state, which is equivalent to the maximum alignment when coupling a pair of  $h_{11/2}$  neutron holes to the  $d_{3/2}$  neutron hole. We note with interest that the beta transitions from the  $^{127}\text{In}$  high spin isomer to these two final states in  $^{127}\text{Sn}$  in practice are of the type  $\pi g_{9/2}^{-1} \rightarrow \nu h_{11/2}^{-1}$ , as discussed further in the next section.

#### D. $A=129$

The data from the  $^{129}\text{In}$  decay showed two  $\gamma$ -ray lines at 281 and 2198 keV with a half-life of about 0.11 s, which is significantly shorter than for other lines in the spectra. The LEP detector spectra also showed the presence of In  $K\alpha$  radiation with the same short half-life. Assuming that the In x rays were excited by internal conversion from the 281 keV transition, we deduce a  $M2$  or  $E3$  multipolarity of which the latter is more probable with regard to the half-life. As reported previously [6], we propose that the 281 keV line is an isomeric transition in  $^{129}\text{In}$ , connecting the expected  $29/2^+$  yrast isomer (formed by a coupling of the  $g_{9/2}$  proton hole to the  $10^+$  core state) to the  $23/2^-$   $\beta$ -decaying isomer studied here. The 2198 keV line is so far unplaced. It could possibly be a transition in  $^{129}\text{Sn}$  following the beta decay of the  $29/2^+$  isomer. However, no supporting evidence for this is seen in the coincidence spectra.

The levels of  $^{129}\text{Sn}$  populated in the  $\beta$  decays of the three isomers in  $^{129}\text{In}$  are shown in Figs. 6–8. All states proposed in the previous  $\beta$ -decay study [7] are confirmed and the combined level scheme has been extended with 18 additional excited states. 78  $\gamma$ -ray transitions were placed in the scheme. Note also in  $^{129}\text{Sn}$  the disagreement between the feeding and depopulating  $\gamma$ -ray intensity for the 1173 keV state.

The neutron hole states ( $d_{3/2}$ ,  $h_{11/2}$ ,  $s_{1/2}$ , and a doublet containing  $g_{7/2}$ ) are identified at 0, 35, 315, and 1865 + 2118 keV, again in agreement with Ref. [7]. Our data show a good candidate for the missing  $d_{5/2}$  state at 1456 keV, which energy agrees well with expectations from systematics.

The four negative parity states from the coupling of the  $h_{11/2}$  neutron hole to the core  $2^+$  level are found in the range 764 to 1360 keV. The level scheme shows six states likely to represent the  $d_{3/2}$  and  $s_{1/2}$  neutron holes coupled to the core phonon at 769, 1047, 1054, 1222, 1288, and 1455 keV. The highest lying of these states probably has a strong component of  $d_{5/2}$  as discussed above, and in similarity to  $^{127}\text{Sn}$ .

At higher energies we are able to identify a few states of 3qp character due to their modes of feeding and decay. The presence of  $\mu\text{s}$  isomers in  $^{129}\text{Sn}$  has long been known, see, e.g., Ref. [7]. In a recent work by Genevey *et al.* [4], two isomeric states were identified at 1761.2 and 1802.2 keV, with half-lives of 3.6 and 2.4  $\mu\text{s}$ , respectively. When gating

on the delayed transitions at 383, 570, 1136, and 1324 keV, the present analysis reveals two components in the TAC spectrum, with half-lives of 3.2 and 2.0  $\mu\text{s}$ , both in agreement with previous results [3,4,7], see Table II and Fig. 2. The  $19/2^+$  and  $23/2^+$  assignments proposed by Pinston *et al.* [3] and Genevey *et al.* [4] are highly plausible and are adopted by us.

These two levels are populated through the  $\beta$  decay of the high spin isomeric state in  $^{129}\text{In}$ . As in  $^{127}\text{In}$ , this isomer should be a member of the  $\pi g_{9/2}^{-1} \nu h_{11/2}^{-1} \nu d_{3/2}^{-1}$  multiplet. The main GT  $\beta$  branch in the decay feeds a level at 3993 keV in  $^{129}\text{Sn}$  with a transition effectively of the type  $\pi g_{9/2}^{-1} \rightarrow \nu g_{7/2}^{-1}$ . Unlike the situation in  $^{127}\text{Sn}$ , we find no trace of a  $\gamma$  transition from the 3993 keV state to the  $15/2^-$  phonon state at 1172 keV. An  $E2$  transition between these states would be of the type  $g_{7/2} \rightarrow d_{3/2}$  and thus allowed by the configurations, but can be forbidden if the states differ too much in angular momenta. The absence of this transition leads us to conclude that the angular momenta of the 3993 keV state and of the  $^{129}\text{In}$  high spin isomer both are one unit higher than for the corresponding states in  $^{127}\text{In}$  and  $^{127}\text{Sn}$ . The  $^{129}\text{In}$  isomer is therefore assigned  $23/2^-$ , which is the maximum alignment of the configuration. The  $\beta$  decay of the isomer can thus populate the  $23/2^+$  and  $19/2^+$  states in  $^{129}\text{Sn}$  with first forbidden and first forbidden unique transitions, respectively. Our data show only the combined transition intensity of about 14% to these final states in  $^{129}\text{Sn}$ . We assume that this number in practice represents the feeding of the  $23/2^+$  state since the unique transition to the  $19/2^+$  level is expected to be at least an order of magnitude weaker. The configurations involved in the initial and final states of this first forbidden decay suggests that the effective  $\beta$  transition is almost purely of the type  $\pi g_{9/2}^{-1} \rightarrow \nu h_{11/2}^{-1}$ , which has never been observed between single particle configurations. Our data permit us to deduce  $\log ft$  values of 6.2 and 5.8 for these transitions in the decays of  $^{127}\text{In}$  and  $^{129}\text{In}$ , respectively. The value obtained for the  $^{129}\text{In}$  transition, which is expected to connect relatively pure three-particle configurations, is likely to give a good estimate of the “true” transition strength and shows that this type of first forbidden transition is rather fast. The observed  $\log ft=5.8$  compares well with the  $\log ft=5.7$  seen [14] for a corresponding transition (between particle-hole states) in the decay of  $^{132}\text{In}$  to the 4848 keV level in  $^{132}\text{Sn}$ . It is probable that the  $9/2^+$  ground states of  $^{127,129}\text{In}$  decay by similar  $\beta$  transitions to the  $11/2^-$  isomers of the Sn nuclei, having transition intensities of the order 5%–15%. These possible transitions cannot be observed due to the strong  $\beta$  radiations from other branches of the In decays.

#### E. Interpretations and discussion

A shell model calculation of the low-lying spectra of  $^{127}\text{Sn}$  and  $^{129}\text{Sn}$  has been carried out using the  $2s_{1/2}$ ,  $1d_{3/2}$ ,  $1d_{5/2}$ , and  $0g_{7/2}$  from the  $N=4$  shell plus the intruder  $h_{11/2}$  from the  $N=5$  shell to define the model space. Starting from a nucleon-nucleon potential derived from modern meson exchange models, this potential is renormalized for the given medium with  $^{132}\text{Sn}$  as a closed shell system, yielding the nuclear reaction matrix  $G$ . The  $G$  matrix is in turn used as the



starting point for a perturbative many-body scheme for deriving effective shell-model interactions, see, e.g., Refs. [15,16]. In Ref. [15] a preliminary calculation was done in a situation where rather few spin values were reasonably well established. In the present work many new assignments are given which make a comparison with theory very interesting. Thus we recalculate  $^{127}\text{Sn}$  and  $^{129}\text{Sn}$  in the same framework with one parameter changed, the energy of the single-particle state  $h_{11/2}$  in  $^{131}\text{Sn}$  from the erroneous value 242 keV to the new experimental value of 65 keV [17]. It is encouraging to see that theory now reproduces the triplet states  $11/2^-$ ,  $3/2^+$ , and  $1/2^+$  in correct order in both cases.

The results are summarized in Table IV for  $^{127}\text{Sn}$  and Table V for  $^{129}\text{Sn}$ . Without any adjustable parameters the theory reproduces a large number of states in both nuclei. In this context, a discrepancy up to 200 keV is considered acceptable. In general, the theoretical values are somewhat higher than the experimental values which may indicate a weak effect from the next  $N=5$  shell showing that  $^{132}\text{Sn}$  is a good closed shell system.

In  $^{127}\text{Sn}$ , there is a disagreement for the first  $7/2^+$  state of about 300 keV. This deviation is also seen for  $7/2^+$  states in other Sn nuclides [15], and one possible reason is that there is too much pairing correlation in the current model. However, of the other  $7/2^+$  states in  $^{127}\text{Sn}$ , three have deviations of less than 100 keV, while the last one shows a deviation of 157 keV. The remaining deviations are 220 keV or less, and will not be discussed here. As for the ordering of the levels, the overall agreement is good.

In  $^{129}\text{Sn}$ , the situation is similar to that of  $^{127}\text{Sn}$ , and the first  $7/2^+$  state is about 200 keV too high. The next two  $7/2^+$  states have small deviations of 100 keV, while the last identified  $7/2^+$  shows a deviation of 680 keV. This could be due to unobserved levels. One uncertainty in this assignment, is that the level at 1047 keV is probably a  $7/2^+$  state, close to the 1054 keV level which here is considered as  $7/2_1^+$ , and if this is the case, the deviations of the higher  $7/2^+$  will be rather large. The  $3/2_1^-$  state shows a deviation of almost 1 MeV, which could be due to an unobserved level, since this deviation is so much larger than the rest. The  $5/2_1^-$ ,  $9/2_1^-$ , and  $13/2_1^-$  have larger deviations of 223, 414, and 344 keV, respectively. The problem of the  $9/2_1^-$  state was also seen in the article by Holt *et al.* [15]. The reason for this is not understood.

In the case of  $^{129}\text{Sn}$ , several other calculations are available. Genevey *et al.* [4] have used the OXBASH code to calculate the high spin states, and the agreement between theoretical and experimental values is generally very good. The main difference between this calculation and the shell model method, is that the OXBASH uses two-body matrix elements of residual interaction extracted from experimental data where it is possible, while the shell model approach starts with the meson exchange. In both cases the agreement with experimental data is quite satisfactory, but it is clear that more precise model calculations are desired.

Recently, results from Genevey *et al.* [18] regarding the level scheme of  $^{129}\text{In}$  have been presented, suggesting a level at 1688 keV having a spin of  $17/2^-$ . This state is an isomer with a half-life of 8.5  $\mu\text{s}$ , and proposed to be a member of the  $\pi g_{9/2}^{-1} \nu (d_{3/2}^{-1} h_{11/2}^{-1})$  multiplet. The results of an OXBASH cal-

TABLE VI. Systematics of  $M2$  and  $E2$  rates from the  $g_{7/2}$  levels, with energies in keV and the  $E2$  rate is 100 in all cases.

A	125	127	129	129
$E$ (keV) ( $E2$ )	1335	1597	1864	2118
$E$ (keV) ( $M2$ )	1362	1602	1830	2083
$M2$ rate	0.33	0.50	0.33	0.42

ulation given in Ref. [18] suggests that the maximum spin member,  $23/2^-$ , of the multiplet is present within a few tens of keV from the  $17/2^-$  state. This result fits quite well with our finding of the isomeric  $23/2^-$  state at  $1630 \pm 56$  keV in  $^{129}\text{In}$ . For  $^{127}\text{In}$ , no excited states has been determined, so a similar discussion is not possible.

Using the present results, several interesting comparisons can be made. The systematics of relative  $M2$  and  $E2$  transition rates from the  $g_{7/2}$  to the  $h_{11/2}$ , and  $d_{3/2}$  levels of  $^{125,127,129}\text{Sn}$  are shown in Table VI. The  $E2$  transition rate has been normalized to 100 in all cases, so only the  $M2$  rate is given explicitly in Table VI. One can note that the relative rates of these single particle transitions are remarkably constant as a function of the mass number.

The half-lives of the  $E2$  isomers in Sn are given in Table II. For the new  $E2$  transition from the 1931 keV level in  $^{127}\text{Sn}$ , we find  $B(E2, 104 \text{ keV}) = 0.40$  W.u. or  $15.2e^2 \text{ fm}^4$  which is somewhat less than observed by Genevey *et al.* [4] for the corresponding transition in  $^{129}\text{Sn}$ . The  $E2$  transition probabilities from the microsecond isomers have been calculated theoretically and are shown in Table VII along with the results from our experiments. The calculated values agree well for  $^{129}\text{Sn}$ , but is somewhat low for the  $23/2^+$  to  $19/2^+$  transition in  $^{127}\text{Sn}$ . When extracting values of the effective neutron charge from the experimental data, the values obtained for  $^{129}\text{Sn}$  are in good agreement with the value of 0.85(3) found for the  $10^+$  to  $8^+$  transition in  $^{130}\text{Sn}$  [19]. The discrepancy between experiment and calculations seen currently for  $^{127}\text{Sn}$  is not unlike the situation reported in Ref. [19] when going from  $^{130}\text{Sn}$  to  $^{128}\text{Sn}$  and may have a similar cause. The  $M2$  transition from the 1827 keV level in  $^{127}\text{Sn}$  has  $B(M2, 732 \text{ keV}) = 0.18 \times 10^{-3}$  W.u. The corresponding, unobserved 589 keV  $M2$  transition in  $^{129}\text{Sn}$  has a partial half-life of more than 100  $\mu\text{s}$ . The  $B(M2)$  is thus less than

TABLE VII. Calculated and experimental  $E2$ -transition probabilities for the  $\mu\text{s}$  isomers, where the experimental values are found assuming an effective charge  $e=1$ . The internal conversion coefficients used are from Rösler *et al.* [20]. The resulting effective charge is also shown.

Transition	Theoretical transition rate ( $e^2 \text{ fm}^4$ )	Experimental transition rate ( $e^2 \text{ fm}^4$ )	Effective charge
$^{127}\text{Sn } 19/2^+ \rightarrow 15/2^+$	70.37	34(3)	0.71(6)
$^{127}\text{Sn } 23/2^+ \rightarrow 19/2^+$	7.43	15.2(20)	1.43(9)
$^{129}\text{Sn } 19/2^+ \rightarrow 15/2^+$	110.2	51(7)	0.69(10)
$^{129}\text{Sn } 23/2^+ \rightarrow 19/2^+$	74.8	50(6)	0.86(8)

about  $0.2 \times 10^{-4}$  W.u. We refer to the work by Pinston *et al.* [3] for a discussion of these  $M2$  transition rates.

#### IV. SUMMARY

In accordance with the expectations, new 3qp isomers have been found in  $^{127}\text{In}$ ,  $^{129}\text{In}$ , and  $^{127}\text{Sn}$ . The  $\beta$ -decaying In isomers are probably  $21/2^-$  in  $^{127}\text{In}$  and  $23/2^-$  in  $^{129}\text{In}$ , have half-lives of  $1.04 \pm 0.10$  and  $0.67 \pm 0.10$  s, respectively, and are located about 1.9 and 1.6 MeV above the ground state. In  $^{127}\text{Sn}$  the 1826 keV isomeric state with a half-life of  $4.8 \pm 0.3$   $\mu\text{s}$  reported by Pinston *et al.* [3] is confirmed, along with a new isomer at 1931 keV decaying into the 1826 keV level, with a half-life of  $1.26 \pm 0.15$   $\mu\text{s}$ . In  $^{129}\text{Sn}$  two isomers

are also seen, in accordance with Genevey *et al.* [4]. The half-lives are  $2.0 \pm 0.2$   $\mu\text{s}$  for the 19.7 keV transition and  $3.2 \pm 0.2$   $\mu\text{s}$  for the 41.0 keV transition. The level schemes constructed agree well with the shell model calculations performed.

#### ACKNOWLEDGMENTS

This work was supported in part by the Norwegian Research Council under Grant No. 133924/432, NorFA, and the TMR program. A. Holt is gratefully acknowledged for discussions regarding the theoretical calculations. H.G. would also like to thank the OSIRIS group at Studsvik for their kind hospitality.

- 
- [1] B. Fogelberg and J. Blomqvist, Nucl. Phys. **A429**, 205 (1984).
  - [2] R. H. Mayer *et al.*, Phys. Lett. B **336**, 308 (1994).
  - [3] J. A. Pinston, C. Foin, J. Genevey, R. Béraud, E. Chabanat, H. Faust, S. Oberstedt, and B. Weiss, Phys. Rev. C **61**, 024312 (2000).
  - [4] J. Genevey, J. A. Pinston, C. Foin, M. Rejmund, H. Faust, and B. Weiss, Phys. Rev. C **65**, 034322 (2002).
  - [5] J. Genevey, J. A. Pinston, H. Faust, C. Foin, S. Oberstedt, and M. Rejmund, Eur. J. Phys. **9**, 191 (2001).
  - [6] B. Fogelberg, H. Mach, H. Gausemel, J. P. Omtvedt, and K. A. Mezilev, in *Nuclear Fission and Fission-Product Spectroscopy*, edited by H. Faust, G. Fioni, S. Oberstedt, and F.-J. Hamsch, AIP Conf. Proc. No. 447 (AIP, Woodbury, NY, 1998), p. 191.
  - [7] L.-E. DeGeer and G. B. Holm, Phys. Rev. C **22**, 2163 (1980).
  - [8] K. Kitao and M. Oshima, Nucl. Data Sheets **77**, 1 (1996).
  - [9] Y. Tendow, Nucl. Data Sheets **77**, 631 (1996).
  - [10] B. Fogelberg, M. Hellström, L. Jacobsson, D. Jerrstam, L. Spanier, and G. Rudstam, Nucl. Instrum. Methods Phys. Res. B **70**, 137 (1992).
  - [11] L. Jacobsson, B. Fogelberg, B. Ekström, and G. Rudstam, Nucl. Instrum. Methods Phys. Res. B **26**, 223 (1987).
  - [12] B. Fogelberg, K. A. Mezilev, H. Mach, V. I. Isakov, and J. Slivova, Phys. Rev. Lett. **82**, 1823 (1999).
  - [13] G. Rudstam, IAEA Report INDC(SWD)-024, IAEA, Vienna, 1993.
  - [14] B. Fogelberg, M. Hellström, D. Jerrestam, H. Mach, J. Blomqvist, A. Kerek, L. O. Norlin, and J. P. Omtvedt, Phys. Rev. Lett. **73**, 2413 (1994).
  - [15] A. Holt, T. Engeland, M. Hjorth-Jensen, and E. Osnes, Nucl. Phys. **A634**, 41 (1998).
  - [16] M. Hjorth-Jensen, T. T. S. Kuo, and E. Osnes, Phys. Rep. **261**, 125 (1995).
  - [17] B. Fogelberg *et al.* (unpublished).
  - [18] J. Genevey, J. A. Pinston, H. R. Faust, R. Orlandi, A. Scherillo, G. S. Simpson, I. S. Tsekhanovich, A. Covello, A. Gargano, and W. Urban, Phys. Rev. C **67**, 054312 (2003).
  - [19] B. Fogelberg, K. Heyde, and J. Sau, Nucl. Phys. **A352**, 157 (1981).
  - [20] F. Rösel, H. M. Fries, K. Adler, and H. C. Pauli, At. Data Nucl. Data Tables **21**, 110 (1978).